5288–5298 *Nucleic Acids Research, 2016, Vol. 44, No. 11* *Published online 29 April 2016*
doi: 10.1093/nar/gkw344

The *Borrelia burgdorferi* telomere resolvase, ResT, anneals ssDNA complexed with its cognate ssDNA-binding protein

Shu Hui Huang and Kerri Kobryn*

Department of Microbiology and Immunology, College of Medicine, University of Saskatchewan Academic Health Sciences Building, 107 Wiggins Rd, Saskatoon, SK S7N 5E5, Canada

Received March 2, 2016; Revised April 15, 2016; Accepted April 18, 2016

ABSTRACT

Spirochetes of the genus *Borrelia* possess unusual genomes that consist in a linear chromosome and multiple linear and circular plasmids. The linear replicons are terminated by covalently closed hairpin ends, referred to as hairpin telomeres. The hairpin telomeres represent a simple solution to the end-replication problem. Deoxyribonucleic acid replication initiates internally and proceeds bidirectionally toward the hairpin telomeres. The telomere resolvase, ResT, forms the hairpin telomeres from replicated telomere intermediates in a reaction with similarities to those promoted by type IB topoisomerases and tyrosine recombinases. ResT has also been shown to possess DNA single-strand annealing activity. We report here that ResT promotes single-strand annealing of both free DNA strands and ssDNA complexed with single-stranded DNA binding protein (SSB). The annealing of complementary strands bound by SSB requires a ResT–SSB interaction that is mediated by the conserved amphipathic C-terminal tail of SSB. These properties of ResT are similar to those demonstrated for the recombination mediator protein, RecO, of the RecF pathway. *Borrelia burgdorferi* is unusual in lacking identifiable homologs of the RecFOR proteins. We propose that ResT may provide missing RecFOR functions.

INTRODUCTION

Borrelia species possess highly segmented genomes, harboring multiple circular and linear replicons. The prototype *Borrelia burgdorferi* B31 genome possesses a linear chromosome and 23 plasmids that are a mix of circular and linear replicons (1–3). The linear replicons are terminated by covalently closed DNA hairpins, structures called hairpin (hp) telomeres (4–6).

Our current understanding of the replication cycle of the linear replicons is that DNA replication initiates internally and proceeds bidirectionally toward the hp telomeres (7,8). Replication around the hp telomeres would produce an inverted repeat dimer joined by replicated telomere (*rTel*) junctions. The resulting intermediate has been replicated, but cannot be segregated to daughter cells, until a specialized DNA breakage and rejoining reaction, referred to as telomere resolution, occurs at the *rTel* junctions. Telomere resolution liberates a pair of linear replicons terminated by hp telomeres. *rTel* junctions are processed *in vivo* and *in vitro* into two hp telomeres (9,10). The essential specialized telomere resolvase that performs this reaction for *Borrelia* is known as ResT (11,12). A similar replication strategy has been demonstrated for the lysogen of the N15 bacteriophage; the N15 prophage exists as a linear plasmid terminated by hp telomeres (13–15).

ResT, and other characterized telomere resolvases, catalyzes telomere resolution by a 2-step transesterification reaction with similarity to that promoted by type 1B topoisomerases and tyrosine recombinases (9,16–20). A detailed view of the reaction mechanism can be found in (21). In the simplest view, the essential role of ResT in the cell cycle would be to resolve dimeric replication intermediates to allow cell division. A prediction of this model is that ResT insufficiency would result in a failure to resolve replicated intermediates, leading either to a filamentous phenotype or to a guillotining of the unresolved intermediates by continued cell division. Recent *in vivo* and *in vitro* results suggest a more complex role.

A *B. burgdorferi* strain with conditional expression of ResT was examined for the effect of ResT depletion (12). Growth arrest occurred 48 h after ResT shutoff. Among several unexpected phenotypes, were arrest of DNA replication at 48 h and the failure of the cells to filament. Starting 24 h after ResT shutoff, unit sized linear DNAs disappeared and became progressively more complex, slowly migrating forms that had a roughly equal mix of hp telomeres and replicated, but unresolved, *rTel* junctions. This suggested the linear plasmids examined were present in partially repli-

*To whom correspondence should be addressed. Tel: +1 306 966 8818; Fax: +1 306 966 4298; Email: kerri.kobryn@usask.ca

cated, and possibly strand-exchanged, forms. The observed arrest of DNA replication suggested that ResT may interact directly, or indirectly, with the DNA replication machinery (12).

An additional report suggested a more complex role, for ResT, in hp telomere metabolism. ResT was found to possess single-strand annealing activity and the ability to promote limited strand exchange between single-stranded DNA (ssDNA) donors and homologous partial duplex DNAs (22). We speculated that these activities could indicate that ResT may be needed to promote daughter strand gap repair in cases where the replisome was unable to fully denature the template DNA near the hp telomere to complete DNA synthesis (22). Daughter strand gap repair is normally promoted by RecA action, mediated by the RecFOR proteins, in the RecF DNA repair pathway (23–26). *B. burgdorferi* possesses RecA, but otherwise lacks identifiable components of the RecF pathway, excepting RecJ, which also participates in mismatch repair (1,27).

In this report, we extend our findings that ResT can promote annealing of complementary ssDNA to show that ResT can promote this reaction with the physiological substrate of ssDNA complexed with its cognate ssDNA binding protein (SSB). Furthermore, we demonstrate that ResT interacts with SSB via the conserved amphipathic C-terminal tail (Ct) of SSB. Eubacterial ssDNA binding proteins serve as general assembly platforms for the recruitment of DNA replication, recombination and repair enzymes to sites of SSB-complexed ssDNA (28). The observed interaction of ResT with SSB and its ability to promote single-strand annealing of SSB complexed ssDNA are properties held in common with the recombinational mediator, RecO, of the RecF pathway.

MATERIALS AND METHODS

DNAs

All oligonucleotides were purchased from Integrated DNA Technologies (IDT). The chromosomally encoded SSB from *B. burgdorferi* B31 (locus BB_0114, protein id number AAC66492.1) was synthesized as a reading frame codon-optimized for expression in *Escherichia coli* K12 and blunt-end cloned into pIDTSMART-AMP and verified by DNA sequencing (purchased from Integrated DNA Technologies). This plasmid was used for subsequent cloning into pET15b for expression in *E. coli*. The sequence of the codon-optimized SSB reading frame and of the oligonucleotides used in this study are presented in the Supplementary Material and Methods section (oligonucleotides in Supplementary Table S1).

Proteins

Antarctic phosphatase was purchased from New England Biolabs and is a heat-labile alternative to alkaline phosphatase. Pronase was purchased from Sigma and is a mixture of several nonspecific endo- and exoproteases derived from *Streptomyces griseus* that digest proteins down to single amino acids.

E. coli SSB (EcSSB) was purchased from Promega. ResT was purified as reported in (16,22). *B. burgdorferi* SSB and SSBΔC5 were made as N-terminal His-tagged versions by amplification from a codon-optimized synthetic gene with primers OGCB643/644 and OGCB643/668, respectively, and were cloned into NdeI/BamHI digested, gel-purified pET15b by digestion of the polymerase chain reaction (PCR) products with NdeI and BamHI, followed by gel purification and ligation. Cloning into pET15b fuses SSB to the N-terminal His-tag present in the expression vector. The expression clones were made, verified by sequencing and archived in strain NEB5α (New England Biolabs). The expression plasmids were transformed into the Rosetta strain (Novagen) for expression. SSB and SSBΔC5 were purified as reported in the Supplementary Material and Methods section.

Oligonucleotide annealing assays

Annealing reactions with 'naked DNA' were performed by mixing 15 nM unlabeled oligonucleotide OGCB665 into reaction buffer (25 mM Tris-HCl, [pH = 8.5], 0.1 mM EDTA and 100 mM NaCl). This mixture was chilled on ice for 2 min, to inhibit the rate of spontaneous annealing. 15 nM 5′-^{32}P-end-labeled oligonucleotide OGCB664 and ResT were added followed by incubation at 30°C. Timepoints were taken by removing 18-μl aliquots, from the 120-μl master annealing reactions to tubes with pre-aliquoted sodium dodecyl sulfate (SDS) stop dye containing excess unlabeled OGCB664 to prevent further annealing after reaction termination. The 5X stop dye contains 100 mM Tris-HCl (pH 7.6), 10 mM $MgCl_2$, 3% SDS, 30% glycerol, 0.024% bromophenol blue and 600-nM unlabeled reporter oligonucleotide.

Samples were deproteinated by addition of load dye supplemented with 50 μg/ml pronase, followed by incubation at 30°C for 15 min, prior to gel loading. Annealing assays with 'SSB-complexed DNA' were performed, as noted above, except with separate pre-incubation of OGCB664 and OGCB665 with 130 nM SSB at 30°C for 5 min. Annealing was initiated by mixing the SSB-complexed OGCB664/665 followed by addition of ResT at the concentration indicated in the figure legends. The incubations were continued at 30°C. Samples were deproteinated, as noted above, prior to gel loading. Electrophoretic analysis was performed on 20 × 20 cm vertical gels with 8% polyacrylamide gel electrophoresis (PAGE) 1XTAE/0.1% SDS at 13 V/cm for 105 min followed by gel drying, exposure of the gels to phosphor screens and analysis on a BioRad FX phosphorimaging machine. Reactions were performed in triplicate and the data were quantitated with BioRad's Quantity One software according to the manufacturer's instructions. Reaction curves and statistics were generated with Prism's GraphPad 6.0.

Plasmid annealing assays

5′-^{32}P-end-labeled pUC19 ssDNA was prepared by BamHI digesting pUC19 DNA followed by dephosphorylation with antarctic phosphatase, and by end-labeling with T4 polynucleotide kinase. Enzymes, adenosine triphosphate and buffer were removed/changed with G-25 Sephadex microspin columns. ssDNA was generated for the annealing

experiments by heat treatment conducted in a PCR machine (99.9°C, 5 min) followed by snap cooling of the denatured DNA in ice water to prevent reannealing. Annealing reactions were performed in 25 mM HEPES (pH 8.2), 2 mM $MgCl_2$, 2 mM DTT and 50 mM NaCl with the concentrations of substrate and protein indicated in the figure legend. The annealing reactions were conducted at 37°C for the times indicated and samples were deproteinated by addition of SDS load dye (see above) to a 1X concentration. Pronase was added to 50 μg/ml followed by an additional 15 min incubation at 37°C. The 0.7% agarose 1X TAE gel was run at 1 V/cm for 15 h. The gels were dried onto Hybond N membranes for autoradioaugraphy.

Data analysis

Initial rate data were analyzed using GraphPad PRISM version 6 for Macintosh. Differences between annealing or strand exchange initial rates were examined using unpaired *t*-tests. $*P \leq 0.05$, $**P \leq 0.01$, $***P \leq 0.001$ and $****P \leq 0.0001$.

Electrophoretic mobility (co)-shift assays

Binding reactions with 15 nM 'naked' 5′-^{32}P-end-labeled 664* were performed in annealing assay buffer (25 mM Tris-HCl [pH 8.5], 0.1 mM EDTA) with 40 mM NaCl by incubation at 20°C for 10 min with the concentration of ResT indicated in the figure legend. The NaCl concentration was adjusted to 100 mM and the incubation was continued for an additional 10 min. SSB-complexed 664* was generated by pre-binding 664* (525 nM nucleotides) with 130 nM SSB in annealing assay buffer with 40 mM NaCl at 20°C for 10 min. The salt concentration was adjusted between 100- and 350 mM NaCl and ResT was added to the noted final concentrations, followed by subsequent incubation at 20°C for 10 min prior to gel loading. The samples were prepared for gel loading by addition of 5X load dye to a 1X concentration. 5X load dye contains 200 mM EDTA (pH 8), 32% glycerol and 0.024% bromophenol blue.

Protein–protein crosslinking

Protein–protein crosslinking was conducted in a buffer containing 25 mM HEPES (pH 8.2), 0.1 mM EDTA and either 100- or 200 mM NaCl. Reactions containing 900 nM SSB and/or 900 nM ResT were incubated at 30°C for 15 min prior to addition of glutaraldehyde to a final concentration of 0.001%. The crosslinking reaction was allowed to proceed at 20°C for 5 min. Excess glutaraldehyde was quenched by addition of Tris-HCl (pH 8.5) to a final concentration of 100 mM prior to gel loading. The samples were prepared for gel loading by addition of 5X SDS-load dye to a 1X concentration followed by denaturation of the samples at 95°C for 6 min. 5X SDS-load dye contains 250 mM Tris-HCl (pH 6.8), 500 mM 2-mercaptoethanol, 10% SDS, 50% glycerol and 0.5% bromophenol blue.

RESULTS

We have previously reported that ResT can promote single-strand annealing reactions and limited strand exchange between single-stranded donor DNA and partial duplex targets (22). Additionally, *B. burgdorferi* lacks the highly conserved RecF pathway (1,29). We were interested to discover whether ResT shared any of the properties of the single-strand annealing protein, RecO, of the RecF pathway, and could, thereby, replace some of the missing functions. To test this we determined if ResT shares RecO's unusual ability to anneal complementary strands bound by cognate ssDNA binding protein (SSB).

ResT promotes single-strand annealing with SSB-complexed ssDNA

We obtained recombinant *B. burgdorferi* SSB by construction of a synthetic mini-gene, codon-optimized for expression in *E. coli*. Expression from an IPTG-inducible T7 RNA polymerase system yields, after Ni-NTA and Heparin Sepharose column chromatography, ∼15 mg of purified (>95%) SSB from 1 l of induced culture (see the Supplementary Material and Methods section). We examined the ability of ResT to promote annealing of complementary single strands complexed with SSB. We used an annealing assay with a pair of complementary 35-nt oligonucleotides (see the Materials and Methods section and Figure 1). Briefly, the assay involves mixing a radiolabeled reporter DNA strand with an equimolar amount of cold complementary strand and following the conversion of the ssDNA into duplex DNA on native PAGE gels. The annealing reactions are terminated by addition of SDS load dye containing pronase and and excess unlabeled reporter oligonucleotide that sequesters any remaining unlabeled complementary strand, freezing the annealing reaction at the point of termination (22,30). The timecourses documented in Figure 1B and C indicate that spontaneous annealing of our model ssDNAs was slow and that pre-incubation with a saturating concentration of SSB yielded a similar slow annealing rate. Addition of 112 nM ResT either to 'naked ssDNA' or 'SSB-complexed ssDNA' annealing reactions yielded stimulated annealing reactions. ResT promoted a faster annealing rate with the SSB-complexed ssDNA than with naked ssDNA at this ResT concentration (Figure 1B and C).

The ResT concentration requirements of annealing reactions with naked ssDNA versus SSB-complexed ssDNA were examined. In reactions with naked DNA substrates there was a gradual increase in the initial rate with increasing ResT concentration (Figure 1D). In contrast, reactions with SSB-complexed substrate DNAs exhibited a saltatory jump in the initial rate at the 112 nM concentration of added ResT with a plateau in the annealing rate with higher concentrations of ResT. As 130 nM SSB was used for the pre-incubation of the oligonucleotides, a roughly equimolar ResT concentration seems to be needed to promote annealing of the SSB-complexed complementary strands. Annealing reactions with the intermediate ResT concentration of 112 nM were significantly faster with SSB-complexed ssDNA than with naked DNA (Figure 1D). The ability of ResT to promote annealing of complementary SSB-complexed oligonucleotides was not particular to the sequence or length of the oligonucleotide substrates tested in Figure 1. A pair of 87-nt oligonucleotide substrates, with the same GC-content as those used for Figure 1, were also good

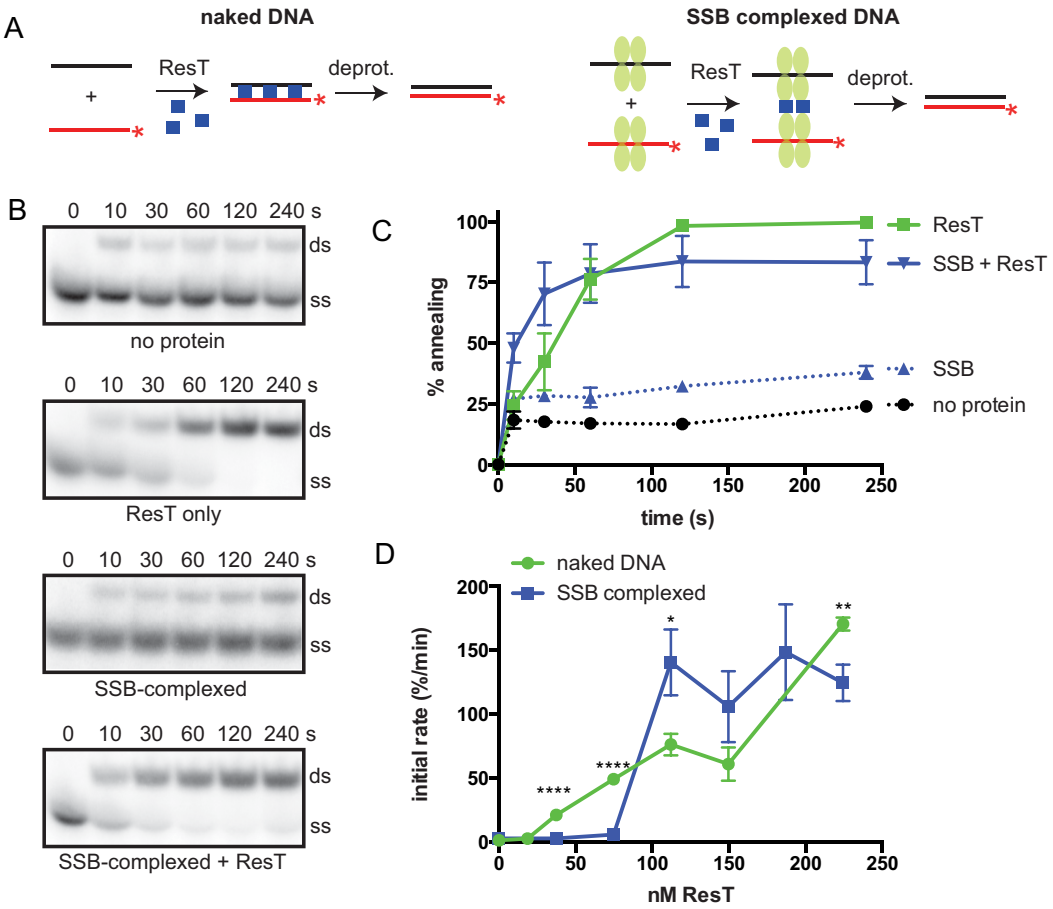

Figure 1. ResT promotes the annealing of complementary single-stranded DNA (ssDNA) complexed with SSB. (**A**) Schematic representation of the single-strand annealing assay. Annealing reactions with 'naked DNA' involve a pair of complementary 35-nt oligonucleotides (OGCB664/665) with one oligo 5′-end-labeled with ^{32}P (asterisk, red/shaded line) partnered with an unlabeled oligo (black line). Addition of ResT (blue/shaded squares) to the complementary oligonucleotides induces annealing. Annealing reactions with 'SSB-complexed DNA' involves the separate pre-incubation of the complementary DNAs with a saturating concentration of SSB (green/shaded ovals), followed by mixing and ResT addition to initiate the annealing reaction. (**B**) Representative 8% PAGE 1X TAE/0.1% SDS gels of reaction timecourses of the indicated annealing reactions. The oligonucleotide substrates were present at 1.05 μM (nucleotides). When used, SSB was present at a saturating 1:8 ratio of protein monomer to nucleotide (130 nM) and ResT was present at 112 nM. (**C**) Shown are % annealing versus time plots of the reactions shown in (B). Reactions were performed in triplicate and the mean and standard deviation are shown. (**D**) The initial rate of annealing is plotted against ResT concentration for reactions performed with naked DNA and SSB-complexed DNA. Reactions were performed in triplicate and the mean and standard deviation are shown. Differences between the initial rates of annealing between naked versus SSB-complexed ssDNA were examined using unpaired *t*-tests. *$P \leq 0.05$, **$P \leq 0.01$, ***$P \leq 0.001$ and ****$P \leq 0.0001$.

substrates for ResT-promoted annealing of both the naked and SSB-complexed forms (Supplementary Figure S1).

The conserved C-terminal tail of SSB is needed for ResT annealing of SSB-complexed ssDNA

We tested if ResT was able to support annealing in reactions where a saturating concentration of EcSSB was used to produce the SSB-complexed substrate (Supplementary Figure S2). ResT was found to be compatible with EcSSB. *B. burgdorferi*'s SSB is clearly identifiable as an EcSSB homolog, but is 29 amino acids shorter and shares less than 30% identity/60% overall similarity with EcSSB, except in the last seven amino acids where the two proteins share (71.4% identity/100% similarity; Supplementary Figure S2B). EcSSB has been documented to interact with DNA replication, replication restart, recombination and repair functions, including DNA pol III (χ subunit), PriA, TopoIII, RecQ, RecO, RecG and ExoI, via this highly conserved amphipathic C-terminal tail (SSB-Ct; (28)). Key to the documented protein–protein interactions are the conserved acidic patch (DDD) and the final hydrophobic residues (28). We deleted the final five residues of SSB that encompass the conserved part of the acidic patch and the final hydrophobic residues, to produce a mutant referred to as SSBΔC5 (Supplementary Figure S2). SSBΔC5 was compared with wild-type SSB in electrophoretic mobility shift assays and by protein crosslinking to determine if the ΔC5 deletion had gross effects on ssDNA binding affinity or SSB oligomerization status. There was little observed difference between the ΔC5 mutant and wild-type SSB (Supplementary Figure S3).

We used the ΔC5 mutant to produce SSBΔC5-complexed ssDNA for annealing reactions. SSBΔC5, in the absence of ResT, supports slow annealing of the 664/665 oligonucleotide pair. ResT promotes a much

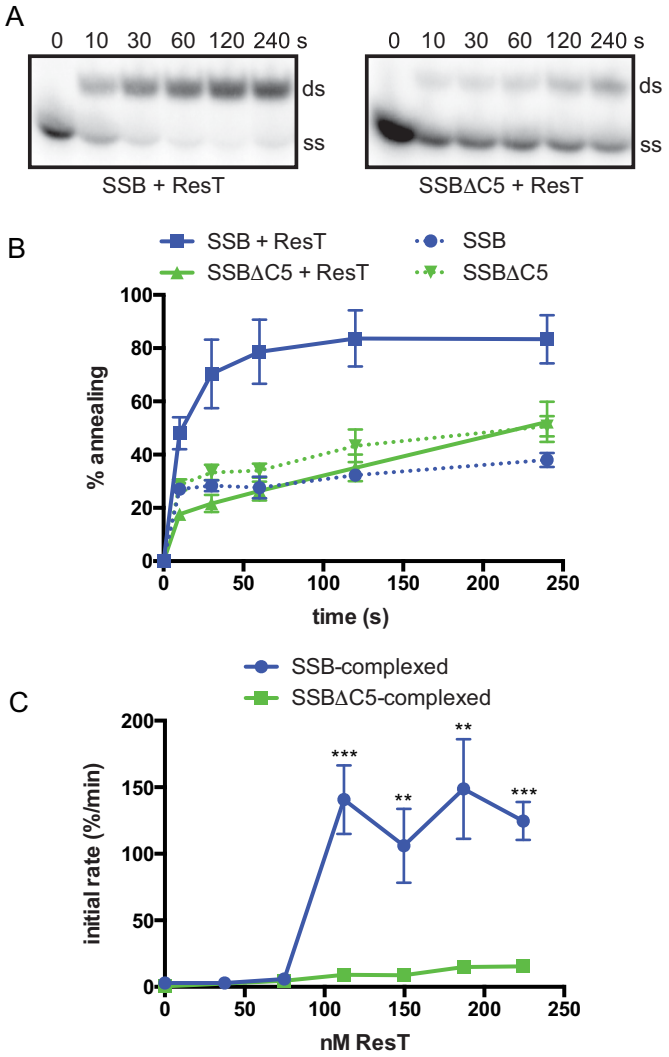

Figure 2. A deletion of the SSB-Ct domain abrogates ResT-promoted annealing of SSB-complexed complementary ssDNA. (**A**) Representative 8% PAGE 1X TAE/0.1% SDS gels of reaction timecourses of the indicated annealing reactions. The oligonucleotide substrates were present at 1.05 μM (nucleotides). SSB or SSBΔC5 was present at a saturating 1:8 ratio of protein monomer to nucleotide (130 nM). ResT was present at a 112 nM concentration in the examples shown. (**B**) Shown are % annealing versus time plots of the reactions shown in (A). Also shown are annealing timecourses with wild-type SSB or SSBΔC5 incubated with the complementary ssDNAs without subsequent ResT addition. Reactions were performed in triplicate and the mean and standard deviation are shown. (**C**) The initial rate of annealing is plotted against ResT concentration for reactions performed with wild-type SSB versus SSBΔC5-complexed ssDNA. Reactions were performed in triplicate and the mean and standard deviation are shown. Differences between the initial rates of annealing between SSB versus SSBΔC5-complexed ssDNA were examined using unpaired *t*-tests. $*P \leq 0.05$, $**P \leq 0.01$ and $***P \leq 0.001$.

slower annealing reaction with SSBΔC5-complexed DNA than with ssDNA bound with wild-type SSB (Figure 2B and C). At the 112 nM ResT concentration documented in Figure 2B, the annealing reaction with the ΔC5 mutant SSB is similar to that of the background annealing rate supported by SSBΔC5 alone. This concentration of ResT is sufficient to drive a robust annealing reaction with the ssDNA bound by wild-type SSB. Increasing the

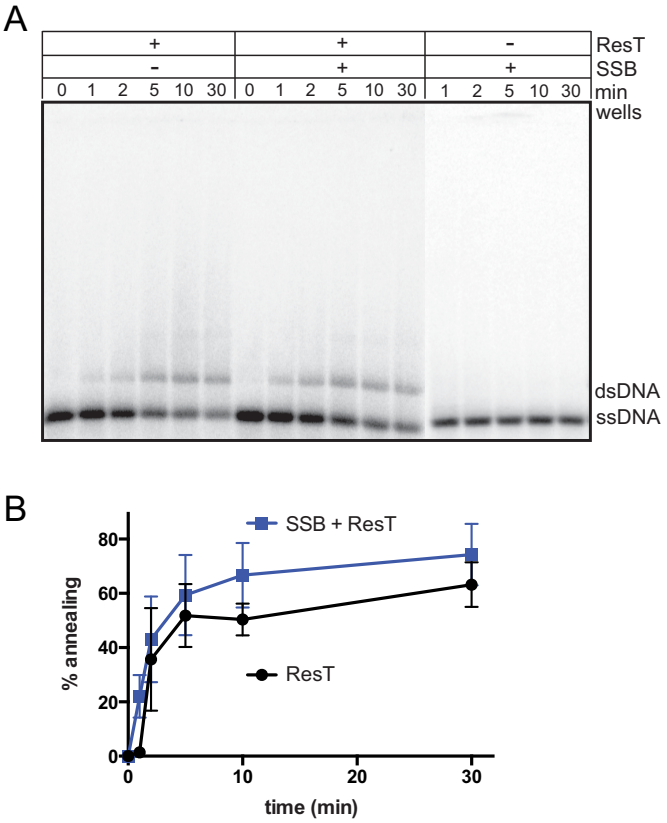

Figure 3. ResT promotes the annealing of plasmid-length ssDNA. Plasmid annealing reactions were carried out with 1.78-μM (nucleotides) 5′-end-labeled, heat denatured, BamHI-digested pUC19 DNA. SSB-complexed ssDNA was generated by pre-incubation with 181 nM SSB followed by addition, where indicated, by addition of ResT (224 nM). Annealing reactions containing only ResT were 'mock' pre-incubated without SSB addition prior ResT addition. (**A**) Representative 0.7% agarose 1xTAE gel analysis of plasmid annealing reactions. The gel migration positions of heat denatured pUC19 (ssDNA) and unit-length duplex (dsDNA) are indicated by the labels to the right of the gel. Reaction timepoints and the proteins present in the reactions are indicated in the gel-loading key above the gel. (**B**) Shown are % total plasmid annealing versus time plots of the indicated plasmid annealing reactions. Shown are the mean and variance of two replicates.

ResT concentration from 75 to 224 nM in the SSBΔC5 reactions resulted in a modest but significant increase in the initial rate of annealing ($P = 0.0102$). In all cases, where annealing of SSB-complexed DNA was supported by ResT, the reactions with SSBΔC5-complexed ssDNA were significantly impaired relative to the reactions using wild-type SSB (Figure 2C) suggesting that the ΔC5 mutation compromises ResT–SSB interactions that promote the annealing reaction.

ResT promotes annealing of plasmid-length ssDNA

We tested if ResT could anneal ssDNA possessing complex secondary structure by assessing the ability of ResT to anneal plasmid-length DNA strands. Additionally, we tested if ResT could anneal plasmid-length ssDNA coated with SSB (Figure 3). Initial assays using the relatively high salt buffer (100 mM NaCl) used in Figures 1 and 2 showed little ResT-promoted plasmid annealing (data not shown).

When the buffer conditions were adjusted to lower the NaCl concentration to 50 mM, ResT-promoted plasmid annealing was readily observed, both on 'naked' and SSB-complexed substrates. Under the saturating SSB concentration and low salt conditions used, SSB displays a highly cooperative mode of binding that results in ssDNA being sequestered in a 'beads-on-a-string' arrangement with SSB, severely restricting its accessibility (31). Despite this sequestration, ResT annealing of the SSB-complexed plasmid-length strands was not significantly different from the annealing seen with 'naked' DNA (Figure 3B). Two categories of annealing products were observed in our gel-based annealing assay, unit-length duplex plasmid and partially annealed products that produce a network of DNAs that smear up the gel toward the wells (32). A much greater fraction of the annealed products were produced as this partially annealed network when a sub-saturating concentration of ResT (112 nM) was used instead of the 224 nM ResT concentration used in Figure 3 (data not shown).

ResT-promoted strand exchange tolerates SSB binding to the donor ssDNA

Our previous report of the single-strand annealing activity of ResT demonstrated that ResT could promote limited strand exchange between single-strand donor DNA and partial duplex targets by virtue of its single-strand annealing activity (22). Strand exchange is initiated by annealing of the donor ssDNA to a single-stranded flank and occurs by 3-strand branch migration within the duplex region (33). It was of interest to determine if this more complicated reaction would tolerate pre-binding the single-stranded donor DNA with SSB. The results are presented in Figure 4. ResT was able to promote strand exchange with SSB-complexed donor (Figure 4B and C). Pre-binding the ssDNA donor with wild-type SSB was well tolerated. Pre-binding with SSBΔC5 significantly reduced the initial rate of strand exchange relative to pre-binding with wild-type SSB, but was still significantly higher than that observed with donor ssDNA pre-incubated with SSBΔC5 without subsequent ResT addition (Figure 4C). With these substrates and reaction conditions, pre-incubation of both the single-stranded donor and the partial duplex target DNA with SSB completely suppressed strand exchange (data not shown).

ResT–SSB interaction

We sought to detect ResT–SSB interactions by use of an electrophoretic mobility co-shift assay (Figure 5). Titration of ResT into binding reactions with the 664 oligonucleotide, used as the radiolabeled strand in the preceding annealing assays, led to a progressive conversion of free 664 into a well-shifted complex (lanes 2–6; Figure 5B). Pre-incubation of 664 with SSB yielded a discrete SSB/ssDNA complex that enters the gels and was progressively converted into a well-shifted complex by titration of ResT into co-binding reactions (lanes 7–12; Figure 5B). To test if the well-shifted complexes, in the ResT/664 versus SSB/664 + ResT reactions, represent different complexes, we tested their sensitivity to NaCl concentration. The ResT + 664 binding reactions produced a wellshift that was resistant to disruption with as much as 350 mM NaCl (lanes 2–6; Figure 5C). Addition of ResT to the wild-type SSB/ssDNA complex, followed by incubation in buffer containing 100 mM NaCl, co-shifted 83% of this complex into the wells (lane 9; Figure 5C). Addition of ResT to the SSBΔC5/ssDNA complex, under the same conditions, co-shifted only 17% of the SSBΔC5/ssDNA complex (lane 14; Figure 5C). ResT addition to wild-type SSB/ssDNA complexes produced a co-shift that was sensitive to moderate concentrations of NaCl. Adjusting the NaCl concentration to 200 mM returned 30% of the co-shifted material back to the SSB/ssDNA complex (lane 12; Figure 5C). The small yield of co-shifted ResT/SSBΔC5/ssDNA complexes obtained in 100 mM NaCl conditions was eliminated by use of 200 mM NaCl conditions (lanes 15–17; Figure 5C). We infer from the differential salt sensitivity of the electrophoretic mobility shifts produced by ResT addition directly to ssDNA versus ResT added to SSB/ssDNA complexes that ResT has not simply replaced SSB on the ssDNA but has produced a distinct complex that contains SSB, ResT and ssDNA. Since the ΔC5 deletion eliminated most of the co-shift, we also infer that the SSB-Ct is involved in the ResT–SSB interaction needed to produce the salt sensitive co-shifts of the SSB/ssDNA complex.

In order to directly visualize ResT interactions with SSB we employed a protein–protein crosslinking approach. Protein–protein crosslinking was induced by addition of glutaraldehyde to incubations containing ResT, SSB, SSBΔC5, ResT/SSB and ResT/SSBΔC5. Initial trials that used glutaraldehyde concentrations sufficient to yield a significant amount of SSB tetramer resulted in crosslinking products with ResT that were too large to enter our SDS-PAGE gradient gels (data not shown). When a sub-saturating glutaraldehyde concentration was used ResT-SSB crosslinks were readily observed (Figure 6). Under these crosslinking conditions, ResT on its own did not multimerize (lane 2; Figure 6A and B). Crosslinking of SSB and ΔC5 yielded dimers, trimers and a trace of the tetrameric form (lanes 4 and 6; Figure 6A and B). When ResT was co-incubated with SSB a ladder of higher molecular weight crosslinking products was seen under buffer conditions containing 100 mM NaCl (lane 8; Figure 6A). An ∼7.5-fold reduction in the yield of these products was seen with the ΔC5 mutant (lane 10; Figure 6A). The results of the electrophoretic co-shift assay indicated that the ResT–SSB interaction was sensitive to a 200-mM concentration of NaCl (Figure 5C). The results of crosslinking assays conducted in buffer containing 200 mM NaCl were qualitatively similar to the 100 mM NaCl results for the individual proteins. Crosslinking reactions with ResT/SSB mixtures conducted in the higher salt buffer showed a greatly reduced yield of ResT-SSB crosslinks and eliminated recovery of ResT-SSBΔC5 crosslinks (lanes 8 and 10; Figure 6B). As DNA was absent from our protein crosslinking assays, the recovery of ResT-SSB protein crosslinks implies that the ResT can interact with SSB in solution. This is consistent with previous studies of SSB interactions with its various binding partners characterized in *E. coli* (28).

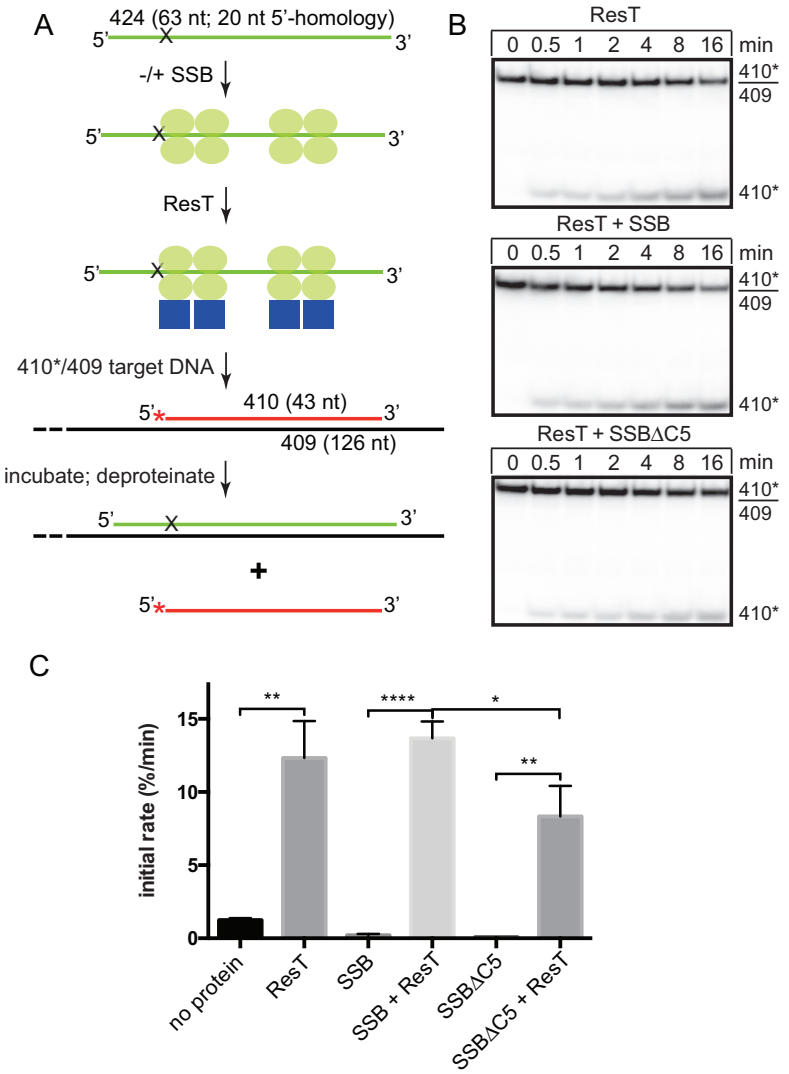

Figure 4. ResT-promoted strand exchange can tolerate SSB binding to the donor ssDNA. (**A**) Schematic representation of the strand exchange assay. ResT promotes strand exchange between a 43-bp partial duplex target DNA (410*/409) and a 63-nt ssDNA donor (424, green/shaded line) with 20 nt of 5′-flank homology with the bottom strand of the partial duplex target. The 424 donor possesses one nucleotide of sequence heterology (X) that falls at the ss-dsDNA junction; this suppresses the relatively high level of spontaneous branch migration when a donor without heterology is used. The top strand of the partial duplex target DNA is red/shaded, the bottom strand black and the red/shaded asterisk indicates a 5′-^{32}P-end-label. In reactions with SSB, the single-stranded donor DNA was pre-incubated with a saturating concentration of SSB. ResT is added and the pre-incubation extended. Strand exchange is initiated by addition of the labeled target DNA (410*/409). Timepoints were withdrawn into stop buffer that terminates the reaction. The reactions were deproteinated by pronase digestion prior to gel loading. The progress of the strand exchange reactions was monitored by visualizing displacement of the 5′-^{32}P-end-labeled strand (410*) from the target DNA on polyacrylamide gels. (**B**) Representative 8% PAGE 1X TAE/0.1% SDS gels of reaction timecourses of the indicated strand exchange reactions. (**C**) Shown are initial rate (%/min) plots of the indicated strand exchange reactions. The oligonucleotide substrates were present at 15 nM (2.19-μM nucleotides present as ssDNA). When used, SSB was present at a saturating 1:8 ratio of protein monomer to nucleotide (274 nM) and ResT was present at 224 nM. Reactions were performed in triplicate and the mean and standard deviation are shown. Differences between strand exchange initial rates were examined using unpaired *t*-tests. *$P \leq 0.05$, **$P \leq 0.01$, and ****$P \leq 0.0001$.

The ResT N-terminal domain is not sufficient to promote annealing of SSB-complexed ssDNA

Our previous report of the single-strand annealing activity of ResT determined that the N-terminal domain of ResT, encompassing the first 163 amino acids, was sufficient to promote single-strand annealing (22). It was of interest to determine if ResT (1-163) was also sufficient to promote annealing of SSB-complexed ssDNA. As shown in Figure 7, ResT (1-163) was able to anneal 'naked' DNA substrates. However, ResT (1-163) was unable to promote annealing of SSB-complexed ssDNA (Figure 7A and B). A preliminary effort to define the region of ResT that interacts with SSB was made by using the ResT (1-163) and ResT (164-449) domains in electrophoretic co-shift and protein–protein crosslinking assays (Supplementary Figures S4 and S5). Consistent with the insufficiency of ResT (1-163) to promote annealing of SSB-bound ssDNA, this domain was found not to interact with SSB. Interestingly, ResT (164-449) was also found to be unable to interact with SSB suggesting that the region of ResT that interacts with SSB must

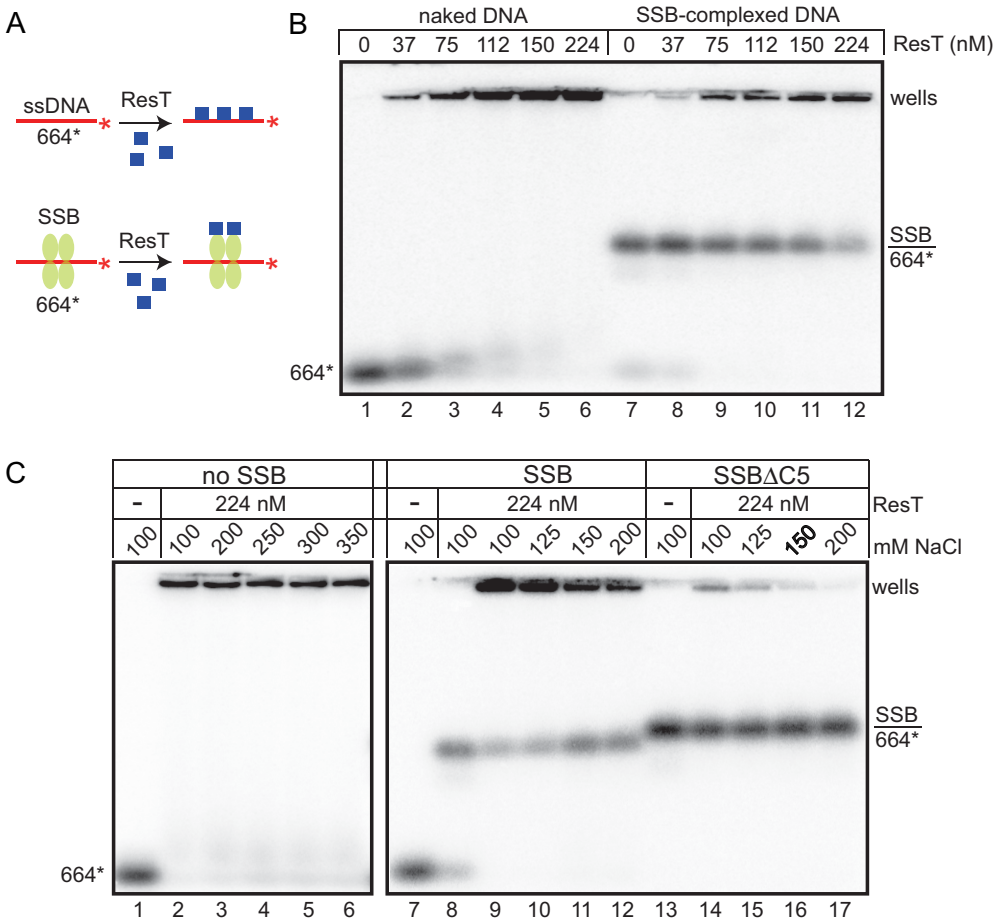

Figure 5. The SSB-Ct domain recruits ResT to SSB/ssDNA complexes. (**A**) Schematic representation of the electrophoretic mobility (co)-shift assay (EMSA) of ResT with naked ssDNA and SSB-complexed ssDNA using a 5′-^{32}P-end-labeled 35-nt oligonucleotide substrate (664*, red/shaded line). The end-label is represented with a red/shaded asterisk. When used, a saturating concentration of SSB was pre-incubated with the 664* oligo; ResT was subsequently added and the incubation continued. ResT binding to naked or SSB-complexed ssDNA was assayed by native agarose gel electrophoresis followed by autoradiography of gels dried to nylon transfer membranes. (**B**) 1.5% agarose 1X TAE gel of EMSAs of ResT with ssDNA and ResT co-shifts of wild-type SSB-complexed ssDNA. Initial ResT or SSB incubation was at 20°C for 10 min in buffer with 40 mM NaCl. Subsequent incubation was at 20°C for an additional 10 min after NaCl was adjusted to a 100 mM concentration by addition of the indicated concentration of ResT and/or ResT storage buffer. Where used, SSB was present at a saturating concentration. (**C**) 1.5% agarose 1X TAE gels of salt challenged EMSAs of ResT with ssDNA and ResT co-shifts of wild-type SSB and SSBΔC5-complexed ssDNA. The binding reactions were performed as indicated for (B) except that 224 nM ResT and various amounts of NaCl were added for the salt challenged co-shifts, with the incubation continuing for an additional 10 min at 20°C.

be formed by contributions from both domains or that the SSB binding site in ResT assumes an altered conformation when not present in the context of the full-length enzyme.

DISCUSSION

In this report we have demonstrated a physical and functional interaction between the *B. burgdorferi* telomere resolvase, ResT and SSB. ResT functions to create the hp telomeres of *Borrelia* through resolution of the *rTel* intermediate (9,12). ResT is also known to possess ssDNA annealing activity (22). Besides promoting the annealing of free DNA strands, we demonstrate that ResT can also promote the annealing of complementary ssDNAs that are complexed with cognate ssDNA binding protein (SSB). As is the case for most previously documented interactions of SSB with proteins involved in genome replication and maintenance, the ResT–SSB interaction appears to be mediated by the conserved amphipathic C-terminal tail of *Borrelia*'s SSB (SSB-Ct).

ResT displays RecO-like properties

Proteins that promote the annealing of complementary ssDNAs can act directly as recombinases in RecA-independent recombination. Single-strand annealing proteins can also be recombinational 'mediators' involved in presynaptic control of strand exchange proteins like RecA or Rad51 (34–36). Examples of single-strand annealing proteins that act directly as recombinases include the phage-derived Redβ/RecT and ERF families of recombinases (37). Paradigm examples of mediators include the eukaryotic Rad52, *E. coli* RecO and T4 UvsY proteins. Recombinational mediators share the properties of (i) promoting the annealing of complementary DNA strands complexed with their cognate ssDNA binding proteins, RPA, SSB and T4 gp32, respectively, for the above examples (38–40); and

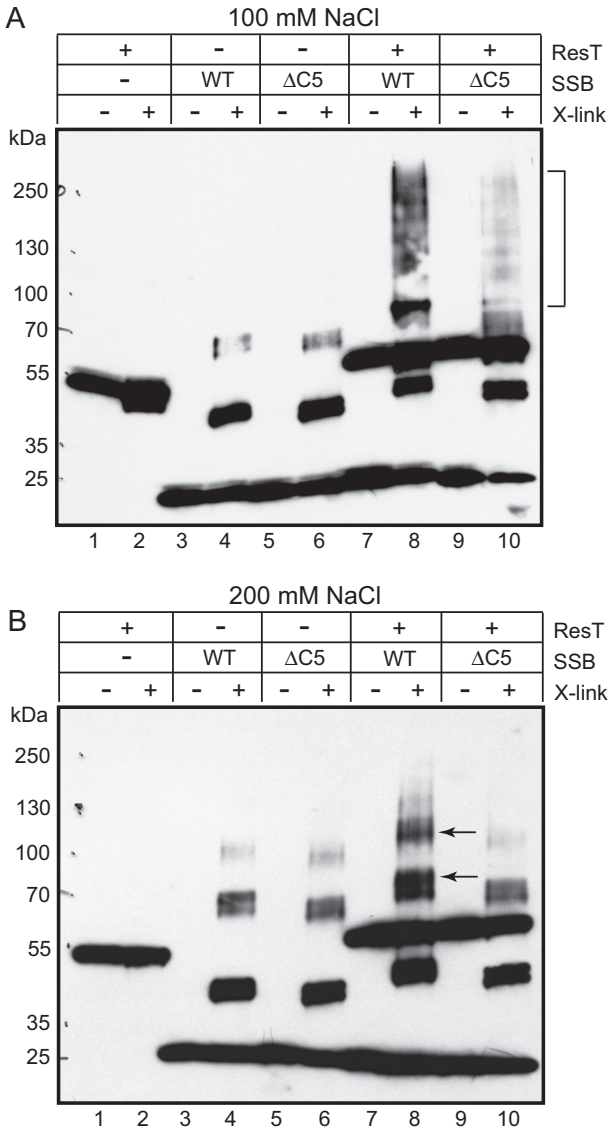

Figure 6. Protein–protein crosslinking with glutaraldehyde captures a ResT-SSB interaction promoted by the SSB-Ct domain. (**A**) Protein crosslinking in buffer conditions with 100 mM NaCl (see the Materials and Methods section for details). The results were visualized by application to a 3.5/4–15% discontinuous SDS-PAGE gradient gel followed by western blotting with a monoclonal antibody that recognizes the N-terminal His-tag present on ResT and SSB. The area of the gel with ResT-SSB crosslinks is indicated by brackets on the right side of the gel. (**B**) Protein crosslinking in buffer conditions with 200 mM NaCl. The gel migration position of the ResT-SSB crosslinks is indicated with arrows.

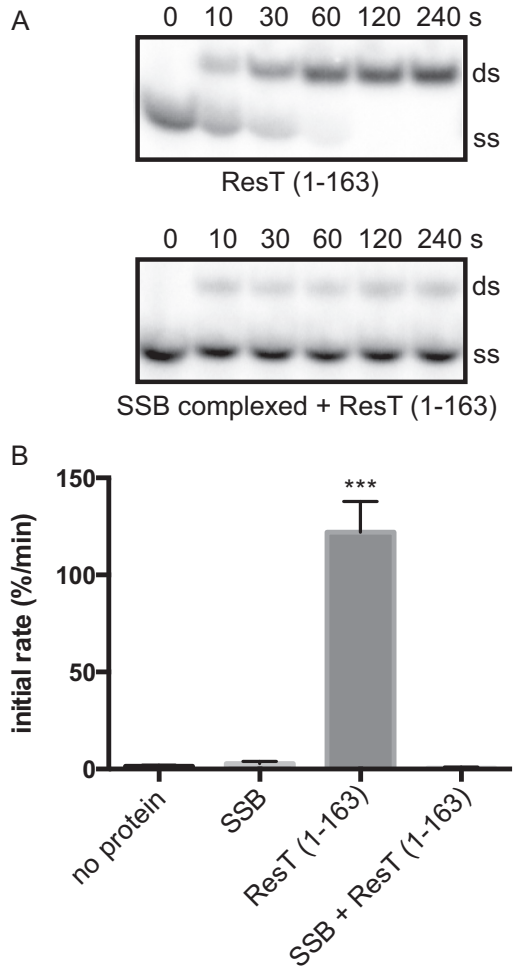

Figure 7. ResT (1-163) promotes annealing of naked ssDNA but not of SSB-complexed ssDNA. (**A**) Representative 8% PAGE 1X TAE/0.1% SDS gels of reaction timecourses of the indicated annealing reactions. The OGCBB664/665 oligonucleotide substrates were present at 1.05 μM (nucleotides). SSB was present at a saturating 1:8 ratio of protein monomer to nucleotide (130 nM). ResT (1-163) was present at a 200 nM concentration in the example shown. (**B**) The initial rate of annealing is shown of mock-incubated reactions, reactions with SSB, ResT (1-163) or ResT (1-163) added to ssDNA pre-bound with SSB. Reactions were performed in triplicate and the mean and standard deviation are shown. Differences between annealing initial rates were examined using unpaired *t*-tests. ***$P \leq 0.001$.

(ii) they aid and stabilize the loading of their cognate recombinase onto ssDNA substrates complexed with ssDNA binding protein (Rad51, RecA and T4 UvsX; (34–36,41)).

Our demonstration that ResT possesses the first property of canonical recombinational mediators raises the possibility that ResT may play a RecO-like role in *Borrelia*. Like ResT, RecO is recruited to ssDNA by an interaction with the C-terminal tail of SSB and this interaction is required for RecO to promote single-strand annealing reactions with substrates bound by SSB (42). *B. burgdorferi* is unusual in not possessing identifiable homologs of the RecFOR and RecQ proteins (1). The RecF pathway mediates RecA-dependent events that contribute to recovery from replication stress and/or DNA damage. Impediments to replication fork progression have different consequences depending upon whether the impediment occurs on the leading or lagging template strands. The replisome can often skip over a lagging strand lesion, leaving in its wake a daughter strand gap (43). Impediments on the leading strand can cause arrest of the replication fork (44). Studies of the genetic requirements, in *E. coli*, of repair of damage caused by UV-irradiation have revealed a role for the RecF pathway both in promoting recombinational repair of daughter strand gaps and in contributing to replication fork processing events that stabilize arrested forks. This allows for rapid recovery of replication after fork arrest (45–47). In both

cases, RecFOR mediates the loading of RecA onto gapped DNA bound by SSB and the DNA pairing activity of RecA is used.

B. burgdorferi is highly unusual in not displaying increased sensitivity to UV-irradiation in strains mutated for a host of recombination and repair functions, including RecA. The only system that has been identified as needed for recovery from UV-irradiation is the nucleotide excision repair system (48). Additionally, many recombination and repair functions, including RecA, are not required for the gene conversion reactions that drive antigenic variation at the *vlsE* locus, though a strong requirement for the RuvAB Holliday junction branch migrase implies some variety of strand exchange reaction is involved (49,50). The most extensively characterized antigenic variation system in bacteria, *pilE* switching in *Neisseria gonorrhoeae*, is dependent upon RecA action in the RecF pathway (51,52). Either these processes are fundamentally different in *B. burgdorferi* or there is a functional alternative to the RecF pathway present. We have previously shown that ResT can promote limited strand exchange reactions between ssDNA donors and partial duplex targets (22). The finding, in this report, that ResT cannot promote these reactions when the ssDNA present in both the donor and partial duplex target DNA is bound by SSB suggests that ResT function may be limited, *in vivo*, to single-strand annealing reactions and possibly mediator function. The product of the λ *orf* gene suppresses *recF*, *recO* and *recR* mutations, demonstrating that RecFOR functions can be provided by a single protein (53).

Further studies will be needed to establish the degree of specificity of ResT for the chromosomal SSB used here and to establish whether the RecO-like properties also extend to ResT mediating the loading of RecA, or other recombinase, onto ssDNA coated with SSB. A related *Borrelia* species that causes relapsing fever, *Borrelia hermsii*, possesses a plasmid-encoded SSB with homology to the *B. burgdorferi* protein studied here. Therefore, some *Borrelia* species or strains may harbor multiple SSB variants (54). Similarly, tests for mediator function in recombinase loading will need to take into account that *B. burgdorferi* possesses not only a chromosomally encoded RecA but also multiple plasmid-encoded copies of an ERF family recombinase (1,2).

SUPPLEMENTARY DATA

Supplementary Data are available at NAR Online.

ACKNOWLEDGEMENT

We would like to thank members of the laboratory for useful discussions.

FUNDING

Natural Sciences and Engineering Research Council of Canada [RGPIN 32 6797-2011]. Funding for open access charge: University of Saskatchewan Publication Fund; Natural Sciences and Engineering Research Council of Canada [RGPIN 32 6797-2011].
Conflict of interest statement. None declared.

REFERENCES

1. Fraser,C.M., Casjens,S., Huang,W.M., Sutton,G.G., Clayton,R., Lathigra,R., White,O., Ketchum,K.A., Dodson,R., Hickey,E.K. *et al.* (1997) Genomic sequence of a Lyme disease spirochaete, *Borrelia burgdorferi*. *Nature*, **390**, 580–586.
2. Casjens,S., Palmer,N., van Vugt,R., Huang,W.H., Stevenson,B., Rosa,P., Lathigra,R., Sutton,G., Peterson,J., Dodson,R.J. *et al.* (2000) A bacterial genome in flux: the twelve linear and nine circular extrachromosomal DNAs in an infectious isolate of the Lyme disease spirochete *Borrelia burgdorferi*. *Mol. Microbiol.*, **35**, 490–516.
3. Chaconas,G. and Kobryn,K. (2010) Structure, function, and evolution of linear replicons in Borrelia. *Annu. Rev. Microbiol.*, **64**, 185–202.
4. Barbour,A.G. and Garon,C.F. (1987) Linear plasmids of the bacterium *Borrelia burgdorferi* have covalently closed ends. *Science*, **237**, 409–411.
5. Baril,C., Richaud,C., Baranton,G. and Saint Girons,I.S. (1989) Linear chromosome of *Borrelia burgdorferi*. *Res. Microbiol.*, **140**, 507–516.
6. Ferdows,M.S. and Barbour,A.G. (1989) Megabase-sized linear DNA in the bacterium *Borrelia burgdorferi*, the Lyme disease agent. *Proc. Natl. Acad. Sci. U.S.A.*, **86**, 5969–5973.
7. Picardeau,M., Lobry,J.R. and Hinnebusch,B.J. (1999) Physical mapping of an origin of bidirectional replication at the centre of the *Borrelia burgdorferi* linear chromosome. *Mol. Microbiol.*, **32**, 437–445.
8. Picardeau,M., Lobry,J.R. and Hinnebusch,B.J. (2000) Analyzing DNA strand compositional asymmetry to identify candidate replication origins of *Borreliaburgdorferi* linear and circular plasmids. *Genome Res.*, **10**, 1594–1604.
9. Kobryn,K. and Chaconas,G. (2002) ResT, a telomere resolvase encoded by the Lyme disease spirochete. *Mol. Cell*, **9**, 195–201.
10. Chaconas,G., Stewart,P.E., Tilly,K., Bono,J.L. and Rosa,P. (2001) Telomere resolution in the Lyme disease spirochete. *EMBO J.*, **20**, 3229–3237.
11. Byram,R., Stewart,P.E. and Rosa,P. (2004) The essential nature of the ubiquitous 26-kilobase circular replicon of *Borrelia burgdorferi*. *J. Bacteriol.*, **186**, 3561–3569.
12. Bandy,N.J., Salman-Dilgimen,A. and Chaconas,G. (2014) Construction and characterization of a Borrelia burgdorferi strain with conditional expression of the essential telomere resolvase, ResT. *J. Bacteriol.*, **196**, 2396–2404.
13. Deneke,J., Ziegelin,G., Lurz,R. and Lanka,E. (2000) The protelomerase of temperate *Escherichiacoli* phage N15 has cleaving-joining activity. *Proc. Natl. Acad. Sci. U.S.A.*, **97**, 7721–7726.
14. Ravin,N.V., Strakhova,T.S. and Kuprianov,V.V. (2001) The protelomerase of the phage-plasmid N15 is responsible for its maintenance in linear form. *J. Mol. Biol.*, **312**, 899–906.
15. Ravin,N.V., Kuprianov,V.V., Gilcrease,E.B. and Casjens,S.R. (2003) Bidirectional replication from an internal ori site of the linear N15 plasmid prophage. *Nucleic Acids Res.*, **31**, 6552–6560.
16. Bankhead,T. and Chaconas,G. (2004) Mixing active site components: a recipe for the unique enzymatic activity of a telomere resolvase. *Proc. Natl. Acad. Sci. U.S.A.*, **101**, 13768–13773.
17. Deneke,J., Burgin,A.B., Wilson,S.L. and Chaconas,G. (2004) Catalytic residues of the telomere resolvase ResT: a pattern similar to, but distinct from tyrosine recombinases and type IB topoisomerases. *J. Biol. Chem.*, **279**, 53699–53706.
18. Kobryn,K., Burgin,A.B. and Chaconas,G. (2005) Uncoupling the chemical steps of telomere resolution by ResT. *J. Biol. Chem.*, **280**, 26788–26795.
19. Briffotaux,J. and Kobryn,K. (2010) Preventing broken borrelia telomeres: rest couples dual hairpin telomere formation to product release. *J. Biol. Chem.*, **285**, 4100–41018.
20. Lucyshyn,D., Huang,S.H. and Kobryn,K. (2015) Spring loading a pre-cleavage intermediate for hairpin telomere formation. *Nucleic Acids Res.*, **43**, 6062–6074.
21. Kobryn,K. and Chaconas,G. (2014) Hairpin Telomere Resolvases. *Microbiol. Spectrum*, **2**, doi:10.1128/microbiolspec.MDNA3-0023-2014.
22. Mir,T., Huang,S.H. and Kobryn,K. (2013) The telomere resolvase of the Lyme disease spirochete, *Borrelia burgdorferi*, promotes DNA

single-strand annealing and strand exchange. *Nucleic Acids Res.*, **41**, 10438–10448.
23. Lavery,P.E. and Kowalczykowski,S.C. (1992) Biochemical basis of the constitutive repressor cleavage activity of recA730 protein. A comparison to recA441 and recA803 proteins. *J. Biol. Chem.*, **267**, 20648–20658.
24. Wang,T.C., Chang,H.Y. and Hung,J.L. (1993) Cosuppression of recF, recR and recO mutations by mutant recA alleles in *Escherichia coli* cells. *Mutat. Res.*, **294**, 157–166.
25. Tseng,Y.C., Hung,J.L. and Wang,T.C. (1994) Involvement of RecF pathway recombination genes in postreplication repair in UV-irradiated *Escherichia coli* cells. *Mutat. Res.*, **315**, 1–9.
26. Morimatsu,K. and Kowalczykowski,S.C. (2003) RecFOR proteins load RecA protein onto gapped DNA to accelerate DNA strand exchange: a universal step of recombinational repair. *Mol. Cell*, **11**, 1337–1347.
27. Schofield,M.J. and Hsieh,P. (2003) DNA mismatch repair: molecular mechanisms and biological function. *Annu. Rev. Microbiol.*, **57**, 579–608.
28. Shereda,R.D., Kozlov,A.G., Lohman,T.M., Cox,M.M. and Keck,J.L. (2008) SSB as an organizer/mobilizer of genome maintenance complexes. *Crit. Rev. Biochem. Mol. Biol.*, **43**, 289–318.
29. Rocha,E.P., Cornet,E. and Michel,B. (2005) Comparative and evolutionary analysis of the bacterial homologous recombination systems. *PLoS Genet.*, **1**, e15.
30. Liu,J., Sneeden,J. and Heyer,W.D. (2011) In vitro assays for DNA pairing and recombination-associated DNA synthesis. *Methods Mol. Biol.*, **745**, 363–383.
31. Lohman,T.M. and Overman,L.B. (1985) Two binding modes in Escherichia coli single strand binding protein-single stranded DNA complexes. Modulation by NaCl concentration. *J. Biol. Chem.*, **260**, 3594–3603.
32. Wu,Y., Sugiyama,T. and Kowalczykowski,S.C. (2006) DNA annealing mediated by Rad52 and Rad59 proteins. *J. Biol. Chem.*, **281**, 15441–15449.
33. Li,Z., Karakousis,G., Chiu,S.K., Reddy,G. and Radding,C.M. (1998) The beta protein of phage lambda promotes strand exchange. *J. Mol. Biol.*, **276**, 733–744.
34. Sung,P. (1997) Function of yeast Rad52 protein as a mediator between replication protein A and the Rad51 recombinase. *J. Biol. Chem.*, **272**, 28194–28197.
35. New,J.H., Sugiyama,T., Zaitseva,E. and Kowalczykowski,S.C. (1998) Rad52 protein stimulates DNA strand exchange by Rad51 and replication protein A. *Nature*, **391**, 407–410.
36. Umezu,K., Chi,N.W. and Kolodner,R.D. (1993) Biochemical interaction of the Escherichia coli RecF, RecO, and RecR proteins with RecA protein and single-stranded DNA binding protein. *Proc. Natl. Acad. Sci. U.S.A.*, **90**, 3875–3879.
37. Iyer,L.M., Koonin,E.V. and Aravind,L. (2002) Classification and evolutionary history of the single-strand annealing proteins, RecT, Redbeta, ERF and RAD52. *BMC Genomics*, **3**, doi:10.1186/1471-2164-3-8.
38. Sugiyama,T., New,J.H. and Kowalczykowski,S.C. (1998) DNA annealing by RAD52 protein is stimulated by specific interaction with the complex of replication protein A and single-stranded DNA. *Proc. Natl. Acad. Sci. U.S.A.*, **95**, 6049–6054.
39. Shinohara,A., Shinohara,M., Ohta,T., Matsuda,S. and Ogawa,T. (1998) Rad52 forms ring structures and co-operates with RPA in single-strand DNA annealing. *Genes Cells*, **3**, 145–156.
40. Kantake,N., Madiraju,M.V., Sugiyama,T. and Kowalczykowski,S.C. (2002) Escherichia coli RecO protein anneals ssDNA complexed with its cognate ssDNA-binding protein: a common step in genetic recombination. *Proc. Natl. Acad. Sci. U.S.A.*, **99**, 15327–15332.
41. Bleuit,J.S., Xu,H., Ma,Y., Wang,T., Liu,J. and Morrical,S.W. (2001) Mediator proteins orchestrate enzyme-ssDNA assembly during T4 recombination-dependent DNA replication and repair. *Proc. Natl. Acad. Sci. U.S.A.*, **98**, 8298–8305.
42. Ryzhikov,M., Koroleva,O., Postnov,D., Tran,A. and Korolev,S. (2011) Mechanism of RecO recruitment to DNA by single-stranded DNA binding protein. *Nucleic Acids Res.*, **39**, 6305–6314.
43. McInerney,P. and O'Donnell,M. (2004) Functional uncoupling of twin polymerases: mechanism of polymerase dissociation from a lagging-strand block. *J. Biol. Chem.*, **279**, 21543–21551.
44. McInerney,P. and O'Donnell,M. (2007) Replisome fate upon encountering a leading strand block and clearance from DNA by recombination proteins. *J. Biol. Chem.*, **282**, 25903–25916.
45. Courcelle,J. and Hanawalt,P.C. (2003) RecA-dependent recovery of arrested DNA replication forks. *Annu. Rev. Genet.*, **37**, 611–646.
46. Courcelle,J., Donaldson,J.R., Chow,K.H. and Courcelle,C.T. (2003) DNA damage-induced replication fork regression and processing in Escherichia coli. *Science*, **299**, 1064–1067.
47. Chow,K.H. and Courcelle,J. (2004) RecO acts with RecF and RecR to protect and maintain replication forks blocked by UV-induced DNA damage in Escherichia coli. *J. Biol. Chem.*, **279**, 3492–3496.
48. Hardy,P.-O. and Chaconas,G. (2013) The nucleotide excision repair system of *Borrelia burgdorferi* is the sole pathway involved in repair of DNA damage by uv light. *J. Bacteriol.*, **195**, 2220–2231.
49. Liveris,D., Mulay,V., Sandigursky,S. and Schwartz,I. (2008) *Borrelia burgdorferi vlsE* antigenic variation is not mediated by RecA. *Infect. Immun.*, **76**, 4009–4018.
50. Dresser,A.R., Hardy,P.-O. and Chaconas,G. (2009) Investigation of the role of DNA replication, recombination and repair genes in antigenic switching at the vlsE locus in *Borrelia burgdorferi*: an essential role for the RuvAB branch migrase. *PLoS Pathog.*, **5**, e1000680.
51. Mehr,I.J. and Seifert,H.S. (1998) Differential roles of homologous recombination pathways in *Neisseria gonorrhoeae* pilin antigenic variation, DNA transformation and DNA repair. *Mol. Microbiol.*, **30**, 697–710.
52. Obergfell,K.P. and Seifert,H.S. (2015) Mobile DNA in the pathogenic Neisseria. *Microbiol. Spectrum*, **3**, MDNA3-0015-2014.
53. Sawitzke,J.A. and Stahl,F.W. (1992) Phage lambda has an analog of Escherichia coli recO, recR and recF genes. *Genetics*, **130**, 7–16.
54. Stevenson,B., Porcella,S.F., Oie,K.L., Fitzpatrick,C.A., Raffel,S.J., Lubke,L., Schrumpf,M.E. and Schwan,T.G. (2000) The relapsing fever spirochete *Borrelia hermsii* contains multiple, antigen-encoding circular plasmids that are homologous to the cp32 plasmids of Lyme disease spirochetes. *Infect. Immun.*, **68**, 3900–3908.